Structural homeomorphism between the electronic charge density and the nuclear potential of a molecular system

Yoram Tal, Richard F. W. Bader, and Jan Erkku
Department of Chemistry, McMaster University, Hamilton, Ontario L8S 4M1, Canada
(Received 1 June 1979)

This paper is a study of the topological relationship between two scalar fields of a molecular system, the electronic charge density and the Coulombic field generated by the atomic nuclei—the nuclear potential. Because of the essential observation that the only local maxima of ground-state charge distributions occur at the positions of the nuclei, the nuclei are the point attractors of the gradient vector fields derived from the charge density and from the nuclear potential. The basins associated with the set of point attractors in either field partition a molecular system into nucleus-dominated regions. The common boundary of any two such neighboring regions contains a particular critical point which generates a pair of gradient paths linking the neighboring attractors. The union of this pair of gradient paths and their end points is called an interaction line. The network of interaction lines defines an elementary graph of the molecular system which identifies the dominant physical interactions in both the charge density and the nuclear potential. Having defined a unique elementary graph for either scalar field for any molecular geometry, the authors partition the total nuclear-configuration space into a finite number of regions. Each region is associated with a particular structure defined as an equivalence class of elementary graphs. The representation of this structural partitioning of nuclear-configuration space is called a structure diagram, which is analogous to a thermodynamic phase diagram. Bader, Nguyen-Dang, and Tal have previously shown that chemical concepts like bonds and molecular structure can be rigorously defined through such a topological analysis of the electronic charge distribution in a molecule. In this paper the authors trace the fundamental role of the nuclear potential in determining the topological properties of this charge distribution. Through a detailed study it is demonstrated that the structure diagrams of the charge density and of the nuclear potential are homeomorphic for the H_2O system. It is conjectured that this homeomorphism exists in general for any molecular system.

I. INTRODUCTION

Within the Born-Oppenheimer approximation, a molecular system is described as some number of electrons moving under the external Coulomb potential $V(\vec{r})$ of the fixed atomic nuclei. The resulting distribution of electronic charge, as described by the charge density $\rho(\vec{r})$, is a real, positive semidefinite function in three-dimensional space. According to a theorem formulated by Hohenberg and Kohn,[1] the ground-state charge density for a given system is uniquely determined by specifying $V(\vec{r})$, and conversely, a particular ground state $\rho(\vec{r})$ determines a unique $V(\vec{r})$, i.e., there exists a unique (but unknown) functional relationship between $\rho(\vec{r})$ and $V(\vec{r})$. Our purpose in this paper is to establish an explicit correspondence between these two scalar fields in terms of their topological properties.

The study of fields in terms of their topological structure is finding an increasing number of applications throughout physics. Although the roots of these ideas are to be found in Faraday's geometrical description of electric and magnetic fields in terms of their lines of force,[2] much of the present stimulus in this direction stems from the modern mathematical analysis of structural stability as employed particularly by Thom.[3] Berry[4] has given a general account to show how Thom's theorem can be used descriptively and predictively to solve problems in wave physics, with particular examples from optics. Berry and Mackley[5] have applied Thom's theory in a study of the streamline patterns in the two-dimensional flows produced in a six-roll mill. Thorndike, Cooley, and Nye[6] have also given a general discussion of the structure and stability of flow fields, classifying the changes in structure for both two- and three-dimensional fields in terms of Thom's list of elementary catastrophes. Collard and Hall[7] have discussed the analysis of the electron density and the Born-Oppenheimer potential energy in terms of their associated gradient vector fields and illustrated the relevance of Thom's theory. Kléman *et al.*[8] have given a classification of topologically stable defects of ordered media, with particular applications to crystals. Coleman and O'Shea[9] have provided a classification for the local topological structure of phase diagrams. Schulman[10] has applied catastrophe theory to the study of phase transitions with tricritical points.

Common to most of the above investigations is the attempt to define the significant structure associated with a phenomenon or a physical system and to

obtain a quantitative description of its stability. Nowhere is the concept of structure more important than it is to the study of molecules. The notion of a molecule being a collection of atoms joined by some network of bonds, i.e., the notion of molecular structure (as distinguished from molecular geometry) plays an essential role in our understanding of chemistry. Owing in large part to the intuitive ideas of Lewis, Pauling, and Slater, the concept of molecular structure has evolved to its point of operational usefulness notwithstanding the fact that it had never been formalized. The deficiencies of such classical structure assignments and their lack of a firm foundation in basic physical concepts are, however, becoming increasingly apparent in, for example, the studies of activated species or chemical intermediates, cluster compounds, and solids.

It has recently been shown[11,12] that the concepts of an atom in the molecule and of a chemical bond find precise expression in terms of the topological properties of the electronic charge density $\rho(\vec{r})$ of a molecular system. As a consequence of these identifications, one is led to a definition of molecular structure and to a phenomenological analysis of structural stability. This approach to the definition of molecular structure and its stability is found to parallel in a most detailed way Thom's general analysis of structure and its stability. The topological properties of $\rho(\vec{r})$ are predominantly determined by the positions of the nuclei which are identified as the *attractors* of Thom's theory. The *basin* associated with each attractor, the space traversed by all the trajectories of $\nabla\rho(\vec{r})$ which terminate at a given attractor, defines the corresponding atom. Consequently, one observes in a molecular system a unique set of trajectories joining pairs of attractors and thereby defining a molecular graph. This molecular graph summarizes the essential topological features of $\rho(\vec{r})$ and provides a basis for a rigorous definition of molecular structure. We show that one may apply the same analysis to the Coulombic field $V(\vec{r})$ and thereby obtain a similar representation of this field in terms of elementary graphs.

In a molecular system the nuclear potential plays a fundamental role in determining the properties of the electronic charge distribution. This point is further elaborated in the present paper by showing the existence of a considerable similarity between the scalar fields $\rho(\vec{r})$ and $V(\vec{r})$. As stressed by Thorndike *et al.*,[6] one may answer the question "when are two fields similar?" by comparing their topological properties. We first demonstrate that the charge density and nuclear potential exhibit structure which is definable in terms of their associated vector fields. We then show that nuclear configuration space may be partitioned into a finite number of regions, each region possessing a unique structure, thereby defining a structure diagram. Finally, we argue that in general, the structure diagrams generated by the charge density and the nuclear potential for a particular system are homeomorphic.

II. ELEMENTARY GRAPHS AND STRUCTURE

Consider the scalar field $f(\vec{r},\vec{X})$ which is a function of the internal variables $\vec{r}\in R^3$ of the *behavior space* and which depends parametrically upon the coordinates $\vec{X}\in R^N$ of the *control space*. In the following discussion the field f may refer to either the electronic charge density $\rho(\vec{r};\vec{X})$ or the external potential $V(\vec{r};\vec{X})$, where

$$V(\vec{r};\vec{X})=\sum_{\alpha} Z_\alpha(|\vec{r}-\vec{X}_\alpha|)^{-1},\quad \vec{X}=\{\vec{X}_\alpha\}. \tag{1}$$

The topological properties of $f(\vec{r};\vec{X})$ are displayed and characterized by its gradient field $\nabla f(\vec{r};\vec{X})$, the gradient being taken with respect to the internal variables $\vec{r}$. For a given value of $\vec{X}$, the vector field $F(\vec{r};\vec{X})=\nabla f(\vec{r};\vec{X})$ generates a one-parameter set of integral curves $\{g_i\}$ called gradient paths, defined by

$$g_i=\left\{\vec{r}(s)\,\middle|\,\frac{d\vec{r}(s)}{ds}=\nabla f(\vec{r};\vec{X}),\quad s\in R,\quad \vec{r}(0)=\vec{r}_i\in R^3\right\}. \tag{2}$$

The topological analysis of $f(\vec{r};\vec{X})$ then proceeds through the search for and the identification of its critical points. A critical point $\vec{r}_c$ is defined by

$$\nabla f(\vec{r},\vec{X})_{\vec{r}=\vec{r}_c}=0. \tag{3}$$

In the neighborhood of a critical point, the field $f(\vec{r};\vec{X})$ is expanded in a Taylor's series, the first nontrivial terms of which are quadratic in the variables $\vec{r}$. The *rank* of the critical point equals the number of nonzero eigenvalues of the Hessian matrix A defined by

$$A_{ij}=\left(\frac{\partial^2 f}{\partial r_i\partial r_j}\right)_{\vec{r}=\vec{r}_c}. \tag{4}$$

Its *signature* is the excess number of positive over negative eigenvalues.[7] The power of catastrophe theory lies in its ability to isolate those discontinuities in a system's behavior which result from continuous changes in its control variables. These discontinuities, which Thom calls catastrophes,[3] are manifest either through the occurrence of critical points of less than maximal rank or through the establishment of a balance between two or more competing regimes. The values of $\vec{X}$ for which $f(\vec{r};\vec{X})$ exhibits singularities, i.e., critical

points of rank less than 3, are catastrophe points of the bifurcation type. Catastrophe points resulting from a balance between competing regimes are called *conflict points*. All other points in R^N are called regular points.

In the neighborhood of $\vec{r}_c$, Eq. (2) becomes

$$\frac{d\vec{r}(s)}{ds} = A(\vec{r} - \vec{r}_c). \tag{5}$$

The nature of the critical point is determined by the sign of the real eigenvalues λ_i of A. Pictorially, the critical point is characterized by its phase portrait—the pattern of trajectories traced out by the gradient paths in its neighborhood. All of the trajectories traced out by the gradient paths originate and terminate at critical points. For critical points of rank 3, four characteristic phase portraits are found, corresponding to the four possible signatures, $-3, -1, +1, +3$. The presence of any of these critical points, labeled as (rank, signature) in the scalar field $f(\vec{r}; \vec{X})$ denotes the presence of a particular element of structure, as we now illustrate.

A. Topology of $\rho(\vec{r};\vec{X})$

We have observed that local three-dimensional maxima in ground-state molecular charge distributions occur only at the positions of nuclei.[11,13] Such maxima correspond to $(3, -3)$ critical points in $\rho(\vec{r}; \vec{X})$[14]; all trajectories of $\nabla\rho(\vec{r}; \vec{X})$ in the neighborhood of a $(3, -3)$ critical point terminate at that point. The concepts of an attractor and its basin as defined in terms of particular sets of trajectories play a central role in Thom's general analysis of structure and its change. It has been shown[12] that the phase portrait of $\rho(\vec{r}; \vec{X})$ in the neighborhood of a nucleus is such that a nucleus fulfills the definition of a point attractor, and the volume of space spanned by the gradient vectors of $\rho(\vec{r}; \vec{X})$ which terminate at the nucleus is its associated basin. Thus a nucleus is a point attractor and the atom is the union of the attractor and its basin. These associations are presented in Fig. 1, which illustrates maps of $\nabla\rho(\vec{r}; \vec{X})$ for charge distributions obtained at several points along the C_{2v} approach of $O(^1D)$ to $H_2(^1\Sigma_g^+)$ to form ground-state water.

The interaction between two such nucleus-dominated regions of space results in the formation of a $(3, -1)$ critical point in $\rho(\vec{r}; \vec{X})$ and the boundary between the regions is determined by the collection of all gradient paths which terminate at the critical point. The positions of the $(3, -1)$ saddle points in $\nabla\rho(\vec{r}; \vec{X})$ are indicated by dots in Fig. 1. Only two gradient paths which terminate at each such saddle point lie in the symmetry plane indicated in this figure. Each such pair of gradient paths defines the boundary between neighboring atoms in this plane. We define the *atomic surface* S_A of an atom A as the boundary of its basin. For an isolated atom, this boundary is found at infinity. Two atoms A and B are neighboring if there exists an *interatomic surface* S_{AB}, defined by $S_{AB} = S_A \cap S_B$ and such that S_{AB} is of dimension 2. Hence $S_A \supseteq \cup_B S_{AB}$.

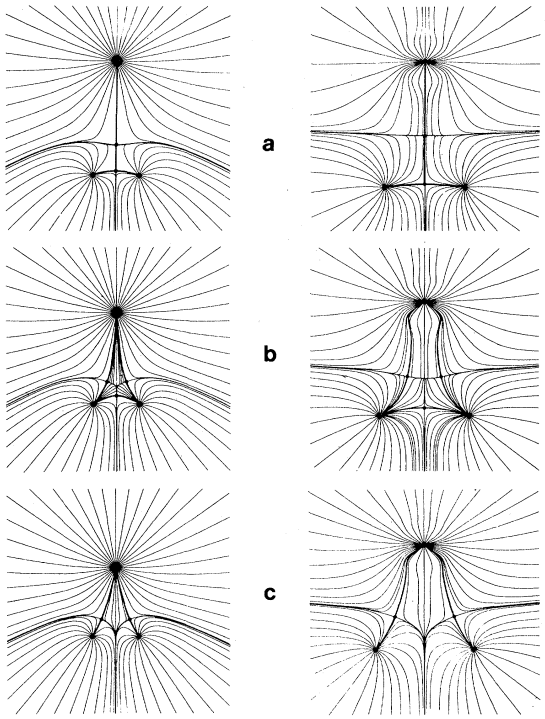

FIG. 1. Gradient maps of $V(\vec{r};\vec{X})$ (left) and of $\rho(\vec{r};\vec{X})$ (right) for symmetric structures of the H_2O system. The elementary graphs are indicated on each diagram by heavy lines, and the (3, -1) critical points by dots.

Two neighboring atoms are linked to one another by the single pair of gradient paths which originate at the $(3, -1)$ critical point, and terminate, one to each, at the neighboring nuclei. These two gradient paths define a line through the charge distribution along which $\rho(\vec{r}; \vec{X})$ is a maximum with respect to any perpendicular displacement. Such lines, called *interaction lines*, are to be found in any scalar field $f(\vec{r}; \vec{X})$ possessing point attractors. In the particular case of the charge density $\rho(\vec{r}; \vec{X})$ they are called bond paths,[11] and neighboring atoms are defined to be bonded to one another. The bond paths are indicated by heavy lines in Fig. 1.

Since atomic nuclei are the only points within a molecular charge distribution which fulfill the definition of an attractor in three dimensions, the set of surfaces generated by the presence of the associated $(3, -1)$ critical points partition the space of a molecule into a collection of chemically iden-

tifiable atoms.[11,12] In addition, it has been demonstrated[11] that the network of bond paths defined by the unique axes of the (3, −1) critical points coincides with the network generated by the linking together of those pairs of atoms which are considered to be bonded to one another on the basis of chemical observations. We define the network of bond paths for a molecule in a given nuclear configuration as the *molecular graph*. In the general case such a network of interaction lines will be referred to as an *elementary graph*.

The two remaining critical points of rank 3 arise as consequences of particular molecular graphs. If three or more nuclei form a ring of bonded atoms, than a (3, +1) critical point must be found within the perimeter of the ring. For such a critical point, two of the eigenvectors of A generate a surface which contains the nuclei and the (3, −1) critical points of the ring. This is a *ring surface* (not an atomic surface) on which $\rho(\vec{r};\vec{X})$ possesses a minimum at the critical point; the gradient paths defining the ring surface originate at the (3, +1) critical point. An example of a bonded ring is shown in Fig. 1.

If four or more nuclei form a bonded cage, a true three-dimensional minimum in $\rho(\vec{r};\vec{X})$ must exist in the interior of the cage; all gradient paths within the cage originate at such a critical point. A three-dimensional minimum in $\rho(\vec{r};\vec{X})$ is a (3, +3) critical point for which all three eigenvalues are positive and hence $\mathrm{Det}A > 0$.

The number and type of critical points of rank 3 which can coexist in a system with a finite number of nuclei are governed by the Poincaré-Hopf relationship. With the structural associations given above, this relationship assumes the form[7]

$$n - b + r - c = 1, \tag{6}$$

where n is the number of nuclei [pseudo-(3, −3)-critical points], b is the number of bonds [(3, −1) critical points], r is the number of rings [(3, +1) critical points], and c is the number of bonded cages [(3, +3) critical points].

B. Topology of $V(\vec{r};\vec{X})$

We now describe the topology of $V(\vec{r};\vec{X})$ and compare it with the topology of $\rho(\vec{r};\vec{X})$. The field $V(\vec{r};\vec{X})$, Eq. (1), becomes infinite if and only if $\vec{r} = \vec{X}_\alpha$, the coordinates of any one of the nuclei. At such a point ∇V is both discontinuous and infinite. Thus the maxima in $V(\vec{r};\vec{X})$, like the corresponding maxima in $\rho(\vec{r};\vec{X})$, are not true (3, −3) critical points. However, again as for $\rho(\vec{r};\vec{X})$ the phase portrait for this point is indistinguishable from that for a true (3, −3) critical point. This behavior is evident in Fig. 1, which portrays maps of the trajectories of $\nabla V(\vec{r};\vec{X})$ for the electronic fields associated with a number of nuclear configurations representing the C_{2v} approach of an oxygen nucleus to two protons held a fixed distance apart. All the trajectories of $\nabla V(\vec{r};\vec{X})$ in the neighborhood of a given nucleus terminate at that nucleus. Thus a nucleus acts as an attractor in both $V(\vec{r};\vec{X})$ and $\rho(\vec{r};\vec{X})$ fields. Moreover, nuclei are the only attractors in $V(\vec{r};\vec{X})$ and they are observed to be the only attractors in (ground-state) charge distributions. Since topological structure and its stability are determined by a state of balance being achieved in the competion between the attractors of a system,[12] one anticipates a significant degree of similarity in the topological properties of ρ and V. Thus one finds that the basins of neighboring attractors in $V(\vec{r};\vec{X})$, as in $\rho(\vec{r};\vec{X})$, are separated by the surface of a (3, −1) critical point and the attractors are linked by an interaction line.

From Fig. 1 it is seen that the same sequence of elementary graphs for the H_2O system is obtained for $V(\vec{r};\vec{X})$ as is obtained for $\rho(\vec{r};\vec{X})$, including a graph corresponding to the bonded ring of nuclei. However, as a consequence of Poisson's equation for $V(\vec{r};\vec{X})$,

$$\nabla^2 V(\vec{r};\vec{X}) = 4\pi \sum_\alpha Z_\alpha \delta(\vec{r} - \vec{X}_\alpha) \tag{7}$$

and the topological properties of $V(\vec{r};\vec{X})$ are constrained relative to those for $\rho(\vec{r};\vec{X})$. Since

$$\nabla^2 V(\vec{r};\vec{X}) = \sum_i \lambda_i , \tag{8}$$

the sum of the eigenvalues λ_i of the Hessian matrix for a critical point in $V(\vec{r};\vec{X})$ other than a (3, −3) must equal zero. No such restriction exists for critical points in $\rho(\vec{r};\vec{X})$. Thus $V(\vec{r};\vec{X})$ may possess both (3, −1) and (3, +1) critical points but with the restriction that $|\lambda_1 + \lambda_2| = |\lambda_3|$, where λ_3 is the eigenvalue of unique sign. It cannot possess a (3, +3) critical point, and hence it cannot exhibit an elementary graph corresponding to a regular cage. However, as discussed later, even in this case $V(\vec{r};\vec{X})$ may possess an elementary graph which is topologically equivalent to a bonded cage of $\rho(\vec{r};\vec{X})$.

A gradient path of V has a simple physical interpretation. It is a line of force—the path traversed by a test charge moving under the influence of the potential $V(\vec{r};\vec{X})$. At a critical point other than a (3, −3) critical point, the force vanishes. Thus a critical point in the field $V(\vec{r};\vec{X})$ denotes a point of electrostatic balance between the attractors of the system. Since the trajectories defining the surface which separates neighboring basins satisfy the "zero-flux" condition

$$\nabla V(\vec{r};\vec{X})\cdot\hat{n}(\vec{r})=0 \quad \forall \vec{r}\in S(\vec{r}), \tag{9}$$

where $\hat{n}(\vec{r})$ is a unit vector normal to the surface S at $\vec{r}$, a test charge on such a surface trajectory is not drawn to either attractor. On the contrary, a test charge lying within a basin is drawn to the attractor and thus the boundary of a given basin defines the region of space dominated by that attractor.

With a common set of elements as attractors, $V(\vec{r};\vec{X})$ exhibits the same basic elements of structure as does $\rho(\vec{r};\vec{X})$, with the atoms and bond paths of the latter field being replaced by the topologically equivalent nuclear basins and nuclear-nuclear interaction lines of the former field. An elementary graph identifies the dominant physical interactions in both $V(\vec{r};\vec{X})$ and $\rho(\vec{r};\vec{X})$. As such it represents the physically essential topological features of either field for any given configuration $\vec{X}$. The elementary graphs form the basis for the definition of structure and structural stability.

C. Structure

So far we have been able to define a unique elementary graph for $\rho(\vec{r};\vec{X})$ or $V(\vec{r};\vec{X})$ for any given value of $\vec{X}$. We also observe that as $\vec{X}$ changes from $\vec{X}_1$ to $\vec{X}_2$ the elementary graph associated with $\vec{X}_2$ may either be equivalent to or different from the one associated with $\vec{X}_1$. This equivalence relationship is defined as follows: the two vector fields $\vec{u},\vec{v}$ defined on R^3 are equivalent, $\vec{u}\sim\vec{v}$, if and only if there exists a homeomorphism which maps the trajectories of $\vec{u}$ onto the trajectories of $\vec{v}$. Hence we define two elementary graphs to be equivalent if the corresponding vector fields $\nabla f(\vec{r};\vec{X}_1)$ and $\nabla f(\vec{r};\vec{X}_2)$ are equivalent. *A structure is therefore defined as an equivalence class of elementary graphs* and may be represented by any elementary graph of the class. We emphasize, however, that while the notion of structure is defined for a general scalar field, molecular structure is specifically determined by the electronic charge density.

From Fig. 1 it is evident that the nuclear potential exhibits the same sequence of structures for the approach of an oxygen nucleus to a pair of hydrogen nuclei as does the charge density for the approach of an oxygen atom to a hydrogen molecule. In fact, we can always find for this system two configurations $\vec{X}_1$ and $\vec{X}_2$ such that the molecular graph of $\rho(\vec{r};\vec{X}_1)$ and the elementary graph of $V(\vec{r};\vec{X}_2)$ are equivalent. Both scalar fields exhibit the same finite set of structures. To complete the comparison of the topological properties of $\rho(\vec{r};\vec{X})$ and $V(\vec{r};\vec{X})$, we must determine the mechanisms of structural change and the nature of structural stability.

III. STRUCTURAL CHANGE AND STRUCTURAL STABILITY

A change in structure is abrupt. We may illustrate this through the sequence of elementary graphs in Fig. 1. Consider the dissociation of the water molecule. As the oxygen nucleus recedes from the protons the system first passes through a series of points in configuration space, all of which possess equivalent elementary graphs as typified by the graph in Fig. 1(c). According to Thom,[3] "if the observer can see nothing remarkable in the neighborhood of a point $\vec{X}$, that is, if $\vec{X}$ does not differ in kind from its neighboring points, then $\vec{X}$ is a regular point of the process." However, at some point along the C_{2v} dissociative path there is a discontinuity in the morphology of the process as evidenced by the sudden appearance of a different kind of elementary graph characteristic of a new structure, the ring structure, Fig. 1(b). The point in configuration space at which this change in structure occurs is a *catastrophe point*. A second abrupt change in structure, a second catastrophe, is encountered when the interaction of the protons with the receding oxygen is reduced to the point where the ring structure is transformed into a structure typified by the graph O–(H_2), Fig. 1(a). We now discuss the mechanisms of structural change.

A. Bifurcation catastrophe

A bifurcation catastrophe occurs when a singularity, i.e., a critical point of rank less than 3, is formed in the scalar field $f(\vec{r};\vec{X})$. In general such a singularity is unstable to a change in the control parameters $\vec{X}$; it may vanish entirely or it may change into two or more critical points of rank 3. The behavior of the system is "catastrophic" in the neighborhood of such a point in configuration space, as a change in the number and nature of the critical points of a system leads to a change in its structure.

The determination of the set of bifurcation points is accomplished through the computation of the behavior surface of the system. For a given field $f(\vec{r};\vec{X})$ with $\vec{r}\in R^3$ and $\vec{X}\in R^N$, the behavior surface is defined by

$$B=\{(\vec{r},\vec{X})\in R^{N+3}\,|\,\nabla f(\vec{r};\vec{X})=0\}. \tag{10}$$

In the particular case of the H_2O system, $\vec{r}=(x,y)$ and $\vec{X}=(D,R)$ (see Fig. 2). The H-H separation is set equal to unity, as all results are readily scaled to any other value. The behavior surface for this system is represented via a set of behavior dia-

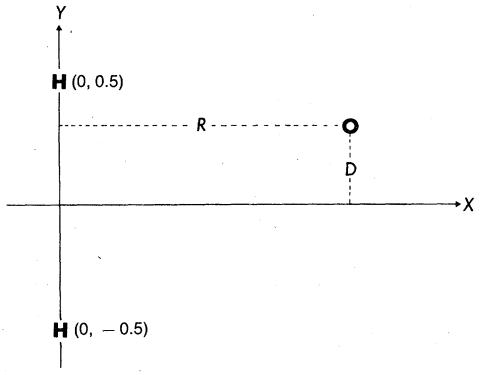

FIG. 2. Definition of the (D,R) control parameters and the (x,y) behavior coordinates for the H_2O system.

grams in which two-dimensional cross sections of the surface are displayed (see Fig. 3).

In Fig. 3(a) ($D=0$), one observed two bifurcation points along the R axis. The values of R at these points, $R_1=2.3043$ and $R_2=1.9187$, thus divide the R axis into three distinct regions: (a) $R>R_1$, in which there are only two (3, −1) critical points and the corresponding structure is O−(H_2), i.e., an interaction line connecting the two hydrogens and another connecting the oxygen to the midpoint of the previous line, as typified by the graphs in Fig. 1(a); (b) $R_2<R<R_1$, in which there are three (3, −1) critical points and one (3, +1) critical point; this region corresponds to a ring structure in which all three nuclei are connected by interaction lines [Fig. 1(b)]; (c) $R<R_2$, in which there are again only two (3, −1) critical points but the structure is H−O−H, i.e., the oxygen is linked to each proton but there is no link between protons [Fig. 1(c)].

The two points in control space, $\vec{X}_1=(0,R_1)$ and $\vec{X}_2=(0,R_2)$, are bifurcation points. At $\vec{X}_1$, a (3, −1) critical point becomes a singularity in $V(\vec{r};\vec{X})$. For a further infinitesimal decrease in R this singularity bifurcates into two (3, −1) critical points and one (3, +1) critical point. As R is decreased still further, the (3, +1) ring critical point moves toward the (3, −1) critical point defining the H-H interaction line. At $\vec{X}_2$ these two critical points merge to form another singularity in $V(\vec{r};\vec{X})$, which for a further infinitesimal displacement along R simply vanishes. Thus the link between the protons is broken by the advance of the oxygen nucleus whose basin, for values of $R<R_2$, extends between the two protons.

The points $\vec{X}_1$ and $\vec{X}_2$ are points of transition between different structures in configuration space. The gradient map for $\vec{X}_1$ is displayed in Fig. 4. The map for $\vec{X}_2$ is shown in Fig. 5 together with

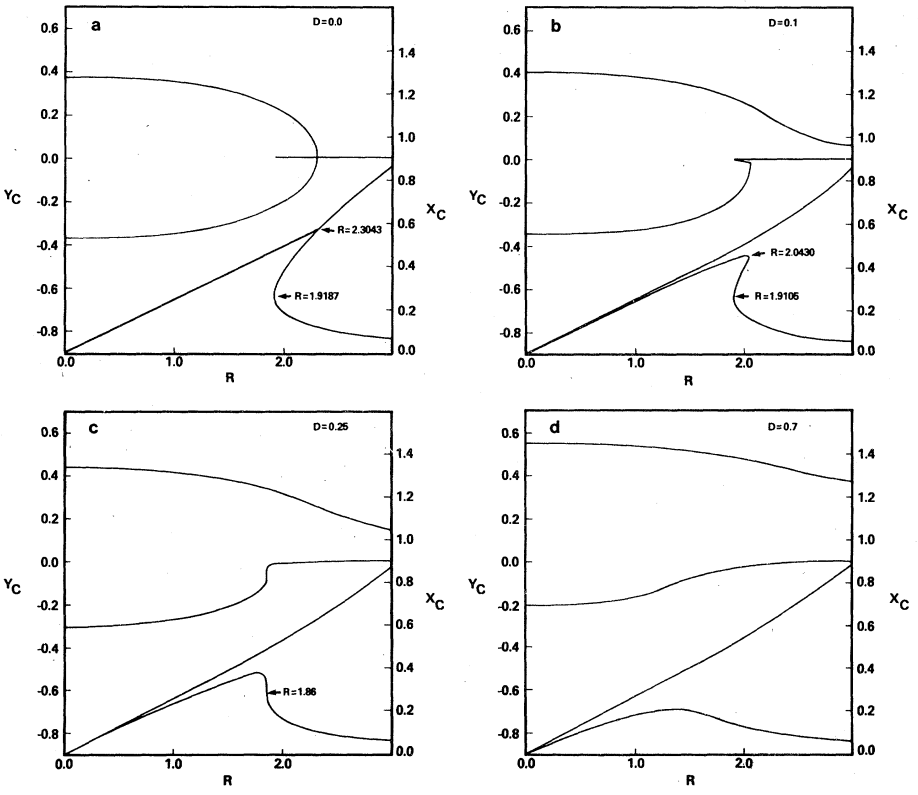

FIG. 3. Behavior diagrams: the (x_c,y_c) coordinates of the (3, −1) and (3, +1) critical points of $V(\vec{r};\vec{X})$ as a function of R for fixed values of D. In each diagram the two uppermost lines refer to y_c, whereas the two bottom lines refer to x_c.

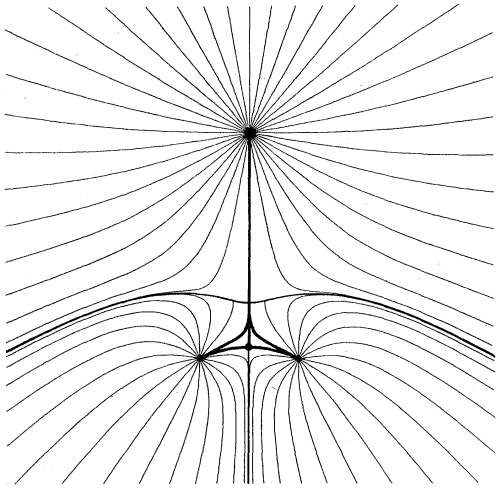

FIG. 4. Gradient map of $V(\vec{r};\vec{X})$ at a catastrophe point on the boundary between the structure ($O-H_2$) and the ring structure.

the corresponding $\nabla\rho(\vec{r};\vec{X})$ map for the molecular system. Comparison of these maps with those in Fig. 1 clearly demonstrates the transitional nature of the bifurcation catastrophes. The structure in Fig. 4 is indeed intermediate between structures 1(a) and 1(b), whereas the structures in Fig. 5 are intermediate between the structures 1(b) and 1(c).

Figure 3(b) displays a behavior diagram for $D=0.1$. The essential features of this diagram are similar to these of Fig. 3(a). Here again, the presence of two catastrophe points, at $R_1=2.0430$ and $R_2=1.9105$, divides the R axis into three structural regions. The only difference is that the region $R>R_1$ corresponds in this case to the structure O–H–H rather than O–(H_2) as found in the case $D=0$. This difference is discussed in Sec. III B. One observes that the ring region is smaller for $D=0.1$ than it is for $D=0$, and that it vanishes for $D>0.25$ [Fig. 3(c) and 3(d)]. Thus for values of

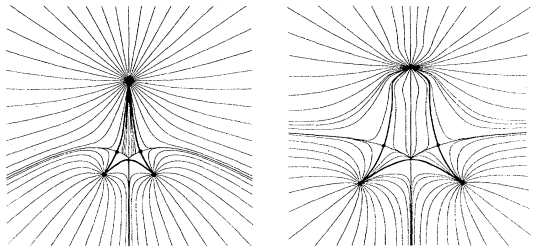

FIG. 5. Gradient maps for $V(\vec{r};\vec{X})$ (left) and $\rho(\vec{r};\vec{X})$ (right) for the symmetrical catastrophe point on the boundary between the regions of ring and open structures of H_2O. The singularities in both $V(\vec{r};\vec{X})$ and $\rho(\vec{r};\vec{X})$ result from the coalescing of the ring critical point with the H–H critical point.

$D>0.25$, all curves of the behavior diagram are single-valued functions of R, implying that the number and kind of critical points exhibited by $V(\vec{r};\vec{X})$ are invariant to changes in R. However, in spite of the absence of bifurcation catastrophe points for values of $D>0.25$, one still encounters structural changes. Examination of the elementary graphs for $D=0.7$, for example, shows that the system undergoes two changes in structure, from O–H–H to H–O–H and back to O–H–H, as R is decreased to zero. A change in structure without change in the kind and number of critical points is the characteristic feature of the second possible mechanism structural change, a conflict catastrophe.

B. Conflict catastrophes

A structural change can occur as a result of a competition between two or more attractors of a system.[3] A conflict catastrophe occurs when the system achieves a state a balance in such a competition.

Examples of such catastrophes points for both the ρ and V fields are illustrated by the elementary graphs given in Fig. 1(a). Such structures are unstable for any change in the value of D. An infinitesimal displacement of the oxygen perpendicular to the C_2 symmetry axis results in a switching of the interaction line (or bond path) from the H–H (3, –1) critical point to the proton lying on the same side of the C_2 axis. Such a displacement yields a new structure of the form O–H–H. Clearly, the intermediate structures in Fig. 1(a) both represent a state of balance in the competition of two neighboring attractors, the protons, for the interaction line from oxygen. One notes that unlike a bifurcation catastrophe, a conflict catastrophe becomes apparent only when structure has been defined over the given field.

The series of graphs shown in Fig. 6(b) illustrates the operation of the conflict mechanism—the switching of attractors—for the case $D=0.7$. These diagrams represent the three structures encountered along the R axis for this value of D. The conflict points are not shown in this case but they clearly exist. Along this path an interaction line switches from a proton to the oxygen nucleus to give the structural change

$$O-H-H \rightarrow H-O-H.$$

At a later stage this process is reversed and the original structure is recovered. Thus the elementary graphs associated with the conflict points along this path are of the form H–(OH). (Because of their inherent instability, it is extremely

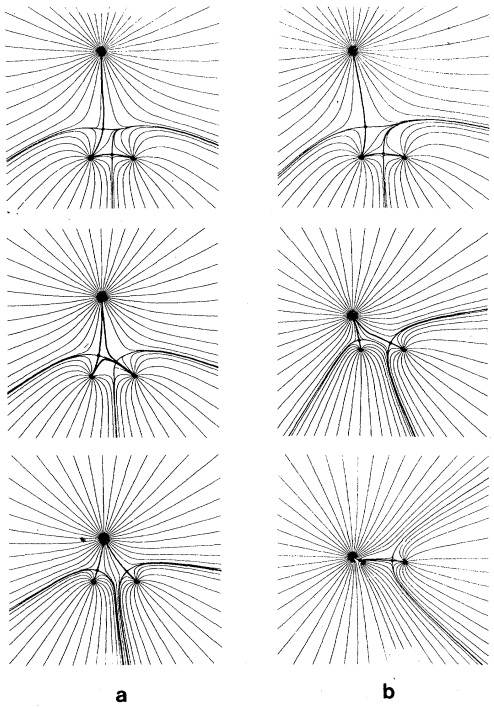

FIG. 6. Gradient maps for asymmetric structures of $V(\vec{r};\vec{X})$: (a) for $D=0.25$ and (b) for $D=0.7$. The central diagram in (a) corresponds to a catastrophe point at the apex of the ring region [Fig. 7(a)]. By suitable displacements from this point the system may attain a ring structure, a conflict structure, or either of the open structures O–H–H and H–O–H. The sequence of structures in (b), beginning with the upper diagram, is O–H–H → H–O–H → O–H–H.

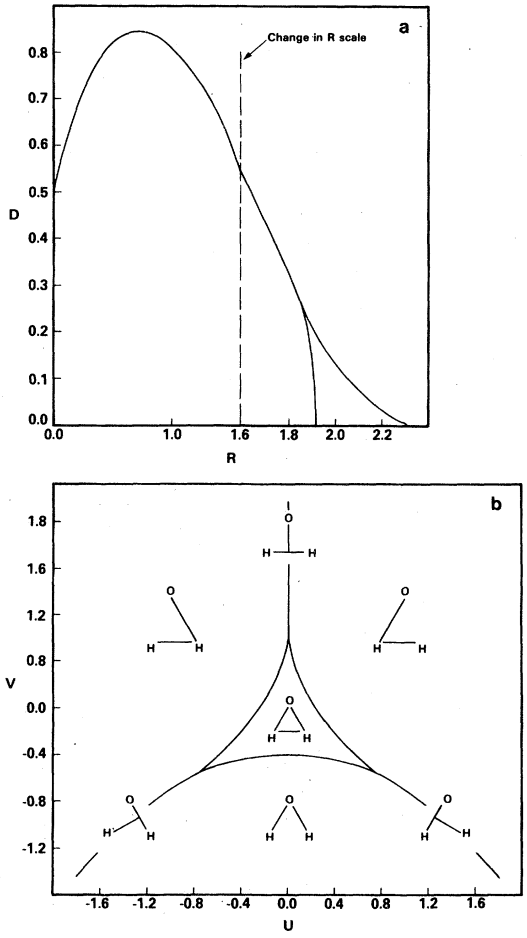

FIG. 7. Structure diagrams obtained from the field $V(\vec{r};\vec{X})$ in the (D,R) control space in (a), and the (u,v) control space, obtained by the linear transformation $u=3.000D$, $v=2.5934(R-1.9187)$, and $w=1$, in (b). In (a) a portion of the conflict-catastrophe set lies on the R axis for values of $R>2.304$. The plot in (a) is the mirror image of that found for negative values of D.

difficult to obtain the molecular graphs associated with assymmetrical conflict points.)

Finally, for $D=0.25$ a "supercatastrophe" is observed. The middle graph in Fig. 6(a) exhibits both bifurcation and conflict behavior. It corresponds to the value of D for which the ring region is reduced to a single point in configuration space [Fig. 3(c)].

C. Structural stability

The collection of all the bifurcation points (the bifurcation set) and the conflict points (the conflict set) forms the catastrophe set in the (D,R) plane. The catastrophe set is a closed subset C of the control space R^N. It partitions the control space into a finite number of structural regions. Each region σ_i is an open subset of R^N such that

$$\forall(i,j),\quad \sigma_i \cap \sigma_j = \emptyset,$$

$$C \cup (\cup_i \sigma_i) = R^N,$$

$$\forall i,\quad \dim\sigma_i = N;\quad \dim C < N.$$

The diagram illustrating this partitioning is called a structure diagram [Fig. 7(a)]. Such a diagram is analogous to a phase diagram in thermodynamics; both represent a partitioning of a control space into structurally stable regions.

Structural stability is defined as follows. Consider a subset $M \subseteq R^N$. A point $\vec{X} \in M$ is structurally stable in M if and only if there exists a neighborhood L of $\vec{X}$ in M such that

$$\forall \vec{X}' \in L,\quad F(\vec{r};\vec{X}') \sim F(\vec{r};\vec{X}),$$

F being the gradient field associated with either $\rho(\vec{r};\vec{X})$ or $V(\vec{r};\vec{X})$. Therefore a point $\vec{X} \in \sigma_i$ is structurally stable in R^N for all i, while a point $\vec{X} \in C$ is structurally unstable in R^N, although it may still be stable in a manifold of dimension less

than N. Indeed, according to this definition of structural stability, a point $\vec{X}\in R^N$ is a conflict point if it is structurally unstable and yet nonsingular. In this way we avoid the use of the so-called Maxwell convention[3] to define the conflict set. Indeed we make a direct use of the notion of structural stability as previously defined.

Through a suitable linear transformation of the control parameters (D,R) to a new coordinate system (u,v) of the control space, the structure diagram of Fig. 7(a) assumes the form shown in Fig. 7(b). The geometry of the bifurcation set in Fig. 7(b) corresponds to a cross section of a hypocycloid. An identical structure diagram is obtained from the scalar field $\rho(\vec{r};\vec{X})$ for the H_2O system.

IV. DISCUSSION AND CONCLUSIONS

We observe that the structure diagrams obtained for $V(\vec{r};\vec{X})$ and $\rho(\vec{r};\vec{X})$ of the H_2O system are homeomorphic in the sense that both exhibit an identical partitioning of the control space yielding the same sets of structures. This homeomorphism may be defined in the following way. To each point of the control space R^N one associates two different functions $f_1=\rho$ and $f_2=V$, and thereby obtains two mappings from R^N onto the function space $C^\infty(R^3,R)$,

$$f_i:\ R^N\to C^\infty(R^3,R),\quad i=1,2.$$

Furthermore, one generates the tangent space $T(R^3)$, a space of vector fields on R^3, by letting the gradient operator act on $C^\infty(R^3,R)$,

$$\text{grad}: C^\infty(R^3,R)\to T(R^3),$$

that is,

$$\forall\vec{X}\in R^N,\quad \forall f_i(\vec{r};\vec{X})=F_i(\vec{r};\vec{X})\in T(R^3),\quad i=1,2.$$

Using these definitions, we define two structure diagrams to be homeomorphic if there exist two homeomorphisms h and t such that the diagram

$$\begin{array}{ccc} R^N & \xrightarrow{f_1} C^\infty(R^3,R) & \xrightarrow{\text{grad}} T(R^3) \\ h\downarrow & & \downarrow t \\ R^N & \xrightarrow{f_2} C^\infty(R^3,R) & \xrightarrow{\text{grad}} T(R^3) \end{array} \tag{11}$$

is commutative, that is,

$$t\circ\text{grad}\circ f_1=\text{grad}\circ f_2\circ h,$$

where $\circ$ denotes a mapping composition. Here the homeomorphisms h and t are defined by

$$\forall\vec{X},\vec{X}'\in R^N\begin{cases} h(\vec{X})=\vec{X}' \\ t\circ F_1(\vec{r};\vec{X})=F_2(\vec{r};\vec{X}'). \end{cases}$$

We have not studied other molecular systems over such a broad range of nuclear configuration space, but have compared the structures of $V(\vec{r};\vec{X})$ and $\rho(\vec{r};\vec{X})$ for many molecules at their equilibrium geometries. In general, equivalent structures are obtained. In some instances the elementary graph for $V(\vec{r};\vec{X})$ must be determined at a geometry other than the equilibrium geometry to obtain an equivalent structure.

We conjecture that the structure diagrams for $V(\vec{r};\vec{X})$ and the ground state $\rho(\vec{r};\vec{X})$ will, in general, be homeomorphic for a particular system. The primary reason for making this conjecture is that $\rho(\vec{r};\vec{X})$ is observed to have the same set of attractors as does $V(\vec{r};\vec{X})$; the topological properties of both fields are controlled and determined by the force fields exerted by the nuclei. As a result of the definition of a nuclear basin, one appreciates even more the dominant role of the nucleus in the determination of the atomic surface defining the boundaries of an atom in a molecular system. In addition to finding the same set of structures for $V(\vec{r};\vec{X})$ and $\rho(\vec{r};\vec{X})$, it has been shown that the mechanisms of structural change are also the same for both scalar fields. Thus the bifurcation and conflict mechanisms appear to describe all possible structural changes in both $V(\vec{r};\vec{X})$ and $\rho(\vec{r};\vec{X})$.

Because of the constraints imposed on $V(\vec{r};\vec{X})$ as a consequence of Poisson's equation [Eq. (7)], the mapping denoted by Eq. (11) does not apply in two particular cases where a structural region is reduced to a single point and therefore becomes a closed subset of R^N. However, the physical equivalence of the structures persists, as we now illustrate. In the H_3^+ system, the ring region of the structure diagram, Fig. 7(b), is reduced to a single point in configuration space.[12] This singleton corresponds to the presence in $\rho(\vec{r};\vec{X})$ of a singularity whose Hessian matrix possesses two zero roots. Because of the conditions implied by Eqs. (9) and (10), $V(\vec{r};\vec{X})$ cannot possess such a singularity. The singularity in $\rho(\vec{r};\vec{X})$ arises from the merging of the $(3,+1)$ critical point of the ring with the three $(3,-1)$ critical points in the perimeter of the ring. Thus it behaves as a threefold degenerate-bond critical point, and the resulting molecular graph is still characterized by three nuclei as in a regular ring structure.

Unlike $\rho(\vec{r};\vec{X})$, $V(\vec{r};\vec{X})$ cannot possess a $(3,+3)$ critical point, for in such a case each $\lambda_i>0$. Thus in the interior of a bonded cage of four nuclei, for example, where ρ possesses a $(3,+3)$ critical point,[15] the corresponding point in V must be a degenerate critical point with three zero roots. Such a critical point results from the coalescing of the $(3,+3)$ cage critical point with the six $(3,-1)$ critical points whose bond paths define the bonds of the cage and with the four ring critical points.

The singularity in $V(\vec{r};\vec{X})$ behaves as does a six-fold degenerate-bond critical point, and the resulting molecular graph is characterized by six bond paths linking the four nuclei as in a regular cage structure. Thus the physical equivalence in the structure observed for $\rho(\vec{r};\vec{X})$ and $V(\vec{r};\vec{X})$, as determined by the equality in the number of their interaction lines and the nuclei they link is maintained even in these particular cases.

The potential-energy operator which determines the electron-nuclear attractive energy for a single electron is $\mathcal{U}(\vec{r};\vec{X}) = -eV(\vec{r};\vec{X})$. Thus an interaction line in an elementary graph of $V(\vec{r};\vec{X})$ represents a minimum energy path in the potential-energy surface, linking two neighboring nuclei. If $V(\vec{r};\vec{X})$ were the sole potential acting in a molecular system, one might expect the electronic charge density to be concentrated along corresponding lines, i.e., the interaction lines of $V(\vec{r};\vec{X})$ would coincide with the bond paths of $\rho(\vec{r};\vec{X})$. In a many-electron system, however, there are electron-electron repulsive forces acting, in addition to the force determined by the external potential. Thus the homeomorphism expressed in Eq. (11) does not, in general, map a point $\vec{X}\in R^N$ onto itself, but rather onto another point $\vec{X}'\neq\vec{X}$. For a given $\vec{X}$ the critical points of $V(\vec{r};\vec{X})$ do not coincide with those of $\rho(\vec{r};\vec{X})$. This is true even for a one-electron system where $V(\vec{r};\vec{X})$ is the sole Coulombic potential, as we now show. In such a case one may obtain from Schrödinger's equation the expression[16]

$$E\rho(\vec{r}) = -\frac{1}{4}\nabla^2\rho(\vec{r}) + \frac{1}{8}\frac{\nabla\rho(\vec{r})\cdot\nabla\rho(\vec{r})}{\rho(\vec{r})} + \mathcal{U}(\vec{r})\rho(\vec{r}) , \tag{12}$$

where

$$\rho(\vec{r}) = \psi^*(\vec{r})\psi(\vec{r}) .$$

Equation (12) may be used to obtain an expression for $\nabla V(\vec{r})$ at a critical point in $\rho(\vec{r})$ [where $\nabla\rho(\vec{r}_c) = 0$]:

$$\nabla V(\vec{r}_c) = -\nabla\mathcal{U}(\vec{r}_c) = -\tfrac{1}{4}\nabla[\nabla^2\rho(\vec{r}_c)]/\rho(\vec{r}_c) . \tag{13}$$

Unless demanded by symmetry, the value of $\nabla^2\rho(\vec{r})$ will not be an extremum at critical points in $\rho(\vec{r})$. Thus V and ρ will not possess critical points at identical $\vec{X}$ values other than at nuclear positions. Therefore, the distribution of electronic charge in a molecular system is not determined entirely by the external force $-\nabla V(\vec{r})$.

Bohm[17] ascribed the stability of a stationary state in a quantum system to the balance of the classical force $-\nabla\mathcal{U}$ by the quantum-mechanical force which is given by the gradient of the "quantum potential." For a one-electron system at a critical point in $\rho(\vec{r})$, Bohm's quantum-mechanical force is just the right-hand side of Eq. (13).

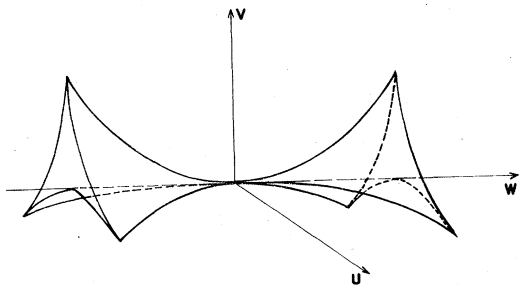

FIG. 8. The bifurcation set of the elliptic umbulic in the (u,v,w) control space.

Finally, we compare our use of the definition of structural stability with that employed by Berry *et al.* in their application of catastrophe theory to the study of diffraction phenomena. The geometry exhibited by the bifurcation set of the structure diagram [Fig. 7(b)] is characteristic of one of the elementary catastrophes, the elliptic umbilic, as described by Thom.[3,12] The unfolding of this elementary catastrophe is a function of two behavior variables (x,y) and three control parameters (u,v,w). In the full control space, the bifurcation set comprises two tapered cones which are joined at the umbilic, the origin of the control space, as illustrated in Fig. 8. The bifurcation set in the structure diagram Fig. 7(b) is a cross section of one of the cones for a value of $w > 0$.[12,18]

Elementary catastrophes provide a description of the caustic surfaces enveloped by families of light rays as observed in diffraction phenomena.[4,19] Berry *et al.*[20] have observed caustics whose structures comprise the elliptic umbilic catastrophe set. For $w \neq 0$ such a caustic is structurally stable: there exists a diffeomorphism corresponding to a smooth reversible mapping which is obtained as w is continuously varied and which leaves the local structure of the caustic unchanged. Such stable caustics are in general found to correspond to one of the elementary catastrophes.[20]

Thus, in the study of diffraction patterns, the stability of a given caustic is related to the genericity of the complete bifurcation set, whereas in our application to molecules the catastrophe set serves to define the different structurally stable regions of the control space. The use by Berry *et al.* of the complete bifurcation set to define the structural stability of the observed caustics is similar to our method of establishing the homeomorphism between the structure diagrams for $\rho(\vec{r};\vec{X})$ and $V(\vec{r};\vec{X})$.

Note added in proof. After this paper was submitted for publication a related work by Parr *et al.* [R. G. Parr, S. R. Badre, and L. J. Bartolotti, Proc. Natl. Acad. Sci. U. S. A. 76, 2522 (1979)] appeared, in which a local model of the relation-

ship between the charge density and the nuclear potential is proposed. Such a local model may be considered a particular case of our general analysis (Sec. IV) where the homeomorphisms h and t in Eq. (11) are replaced by identity mappings. In this case the structure diagrams of ρ and V coincide. The same is true for *any* local model regardless of the detailed functional relationship between V and ρ—provided it is sufficiently smooth and well behaving. In general, however, it is unlikely that a local model of this kind will closely approximate a real system, since not even for the single-electron case [Eqs. (12) and (13)] does one obtain an identical set of critical points for both V and ρ at any given $\vec{X}$.

ACKNOWLEDGMENT

We wish to thank Mr. T. Tung Nguyen-Dang for his careful reading of the manuscript, and for clarifying some points in the topological analysis.

[1]P. Hohenberg and W. Kohn, Phys. Rev. B 136, 864 (1974).

[2]M. Faraday, Exp. Res. 3284. A quotation from this article, which is also quoted by C. Maxwell in *The Scientific Papers of J. C. Maxwell*, edited by W. D. Niven (Dover, New York, 1965), Vol. II, p. 319, is "It would be a voluntary and unnecessary abandonment of most valuable aid if an experimentalist, who chooses to consider magnetic power as represented by lines of magnetic force, were to deny himself the use of iron filings. By their employment he may make many conditions of the power, even in complicated cases, visible to the eye at once, may trace the varying direction of the lines of force and determine the relative polarity, may observe in which direction the power is increasing or diminishing, and in complex systems may determine the neutral points, or places where there is neither polarity nor power (critical points of present theory) even when they occur in the midst of powerful magnets. By their use probable results may be seen at once, and many a valuable suggestion gained for future leading experiments."

[3]René Thom, *Structural Stability and Morphogenesis* (Benjamin, Reading, Mass., 1975).

[4]M. V. Berry, Adv. Phys. 25, 1 (1976); see also M. V. Berry, J. Phys. A 10, 2061 (1977); J. F. Nye, Proc. R. Soc. London A 361, 21 (1978).

[5]M. V. Berry and M. R. Mackley, Philos. Trans. R. Soc. London 287, 1 (1977).

[6]A. S. Thorndike, C. R. Cooley, and J. F. Nye, J. Phys. A 11, 1455 (1978).

[7]K. Collard and G. G. Hall, Int. J. Quantum Chem. 12, 623 (1977).

[8]M. Kléman and L. Michel, Phys. Rev. Lett. 40, 1387 (1978); M. Kléman, L. Michel, and G. Toulouse, J. Phys. Paris Lett. 38, L-195 (1977); G. Toulouse and M. Kléman, *ibid.* 37, L-149 (1976).

[9]A. J. Coleman and D. B. O'Shea, Phys. Rev. B (to be published).

[10]L. S. Schulman, Phys. Rev. B 7, 1961 (1973).

[11]R. F. W. Bader, S. G. Anderson, and A. J. Duke, J. Am. Chem. Soc. 101, 1389 (1979).

[12]R. F. W. Bader, T. T. Nguyen-Dang, and Y. Tal, J. Chem. Phys. 70, 4316 (1979).

[13]In many-electron systems, the observation that local maxima in the electronic charge density are restricted to nuclear positions appears to hold true for excited states as well as for ground states (Ref. 11).

[14]Because of the electron-nuclear coalescence cusp condition ψ [T. Kato, Commun. Pure Appl. Math. 10, 151 (1975)], $\nabla\rho(\vec{r})$ is undefined at a nuclear position, and hence such maxima in $\rho(\vec{r})$ are not true $(3,-3)$ critical points. However, the phase portrait generated by a nuclear maximum is indistinguishable from that characterizing a $(3,-3)$ critical point.

[15]R. F. W. Bader, Y. Tal, S. G. Anderson, and T. T. Nguyen-Dang, Isr. J. Chem. (to be published).

[16]R. F. W. Bader and H. J. T. Preston, Int. J. Quantum Chem. 3, 327 (1969).

[17]D. Bohm, Phys. Rev. 85, 166 (1952).

[18]While the interpretation of the parameters (u,v) is relatively easy, w is more difficult to interpret. In dealing with the charge density, w may be to some extent considered as a "chemical parameter." That is, the catastrophe sets of different triatomic molecules correspond to different values of w. In the case of the nuclear potential w amount to a scaling factor, since the catastrophe set corresponding to any H–H distance can be linearly transformed into the present one [Fig. 7(b)] by normalizing all the coordinates to $R(\text{H–H})=1$.

[19]T. Poston and I. Stewart, *Catastrophe Theory and It's Applications*, (Pitman, London, 1978).

[20]M. V. Berry, J. F. Nye, and F. J. Wright, Philos. Trans. R. Soc. A (to be published).